

Co- and Cu-Doped Titanates: Toward a New Generation of Catalytic Converters

A. Glisenti · M. M. Natile · S. Carlotto ·
A. Vittadini

Received: 20 February 2014 / Accepted: 9 June 2014 / Published online: 1 July 2014
© Springer Science+Business Media New York 2014

Abstract $\text{SrTi}_{0.7}\text{Co}_{0.3}\text{O}_3$, $\text{SrTi}_{0.7}\text{Cu}_{0.3}\text{O}_3$, $\text{SrTi}_{0.7}\text{Co}_{0.15}\text{Cu}_{0.15}\text{O}_3$ were prepared by the “citrate route” and characterized (XRD, XPS, SEM, TPR). Their reactivity with respect to CO oxidation and NO reduction was investigated and compared with that of $\text{CuO}/\text{SrTi}_{0.7}\text{Co}_{0.3}\text{O}_3$ nanocomposite. High conversions were obtained in CO oxidation (90 % at 350 °C for $\text{SrTi}_{0.7}\text{Co}_{0.3}\text{O}_3$). Only $\text{CuO}/\text{SrTi}_{0.7}\text{Co}_{0.3}\text{O}_3$ was observed to be active in NO reduction (100 % at 350 °C).

Keywords Titanates · CO oxidation · NO reduction · Nanocomposites · TWC

1 Introduction

Conventional three-way catalysts (TWCs) are required to be extremely efficient in the reduction of nitrogen oxides and in the oxidation of CO and unburned hydrocarbons. Cost considerations as well as the need to develop catalysts highly effective toward lean-burn exhaust emissions suggest to consider alternative approaches and materials. Perovskite based oxides have been studied as promising alternatives to noble metal catalysts for automotive emission control since 1970s. ABO_3 oxides exhibit good

catalytic activity for CO and HC oxidation reactions: La-based cobaltates and manganites appear to be among the best-performing [1–5]. These perovskite catalysts show good activities for CO and HC oxidation but their efficiency in NO_x elimination is often rather poor.

In principle, A and B sites doping inducing the formation of structural defects (anionic or cationic vacancies) and different oxidation states (in the B site) can be fundamental for the catalytic activity [3, 6–12]. Perovskites are particularly interesting because their properties and reactivity can be tuned by means of doping [13]. On the basis of the reaction mechanisms [14] the perovskite has to be built so to be able to promote CO and hydrocarbons oxidation (and thus the oxygen mobility/exchange) and the dissociative interaction of NO. Surface anion vacancies are also suggested to play a key role. Following this strategy several systems have been investigated as catalysts for the reaction between NO and CO or between NO and hydrocarbons [15–24]. In all these perovskites the A cation is usually a Rare-Earth Element (REE, typically lanthanum) whereas very few efforts have been done to obtain REE-free perovskites active in TWC reactions. In this respect, very few studies concerning titanates have been carried out and focus on the activity of iron titanates in NH_3 -selective catalytic reduction [25, 26] and of Cu doped strontium titanate for diesel soot combustion by NO and O_2 . [27] Doped SrTiO_3 , in particular, seems to be a valuable starting point for NO_x treatment. [28–33]. The aim of the manuscript is to investigate the possibility of obtaining by means of doping, SrTiO_3 -based catalysts active in the TWC reactions, with particular reference to the NO reduction. To this end we selected cobalt and copper as the doping active cations. Cobalt has been considered due to its high activity in oxidation reactions whereas copper is more significant in reduction reactions [29].

A. Glisenti (✉) · S. Carlotto
Dipartimento di Scienze Chimiche, Università degli Studi di
Padova, Via F. Marzolo 1, 35131 Padua, Italy
e-mail: antonella.glisenti@unipd.it

M. M. Natile · A. Vittadini
CNR-IENI, Padua, Italy

2 Experimental

2.1 Synthesis

Samples were prepared by the citrate method starting from $\text{Sr}(\text{NO}_3)_2$, (Sigma-Aldrich 99.9 %), Ti (Sigma-Aldrich 99.9 %), CuO (Strem Chemicals 99.999 %) and CoO (Strem Chemicals 99.999 %). Citric acid monohydrate (Sigma-Aldrich >99 %) is added to an aqueous solution of the cations [obtained by mineralization of CuO and CoO with nitric acid and treatment of Ti with HCl 37 % (Sigma-Aldrich)] with a molar ratio of 1.9:1 with respect to the total amount of cations. Then the solution is heated up to 80 °C in air to promote water evaporation and to obtain a wet-gel. The gel is heated to 400 °C (0.5 °C/min heating rate) for 2 h in air to decompose the organic framework. At the end of the heat treatment, the powder is grinded and calcined at 950 °C, for 6 h. The same procedure was adopted for the synthesis of undoped SrTiO_3 .

The nanocomposite ($\text{CuO}/\text{SrTi}_{0.7}\text{Co}_{0.3}\text{O}_3$) was obtained by wet impregnation of $\text{SrTi}_{0.7}\text{Co}_{0.3}\text{O}_3$ with an aqueous solution obtained by mineralization of CuO with HNO_3 . The obtained suspension was maintained under stirring for 2 days and then kept in rest for 1 day. Water was evaporated in air and the obtained solid was dried at 110 °C for 1 h and at 500 °C for 5 h (in air).

2.2 Characterization

XPS measurements were carried out with a Perkin Elmer Φ 5600 ci Multi Technique System. The spectrometer was calibrated by assuming the binding energy (BE) of the Au $4f_{7/2}$ line to be 84.0 eV with respect to the Fermi level. Both extended spectra (survey—187.85 eV pass energy, 0.5 eV/step, 0.05 s/step) and detailed spectra (for Sr 3d, Ti 2p, Cu 2p, Co 2p, O 1s and C 1s—23.5 eV pass energy, 0.1 eV/step, 0.1 s/step) were collected with a standard Al $K\alpha$ source working at 250 W. The standard deviation in BE values of the XPS line is 0.10 eV. The atomic percentage, after a Shirley-type background subtraction, [34] was evaluated by using the PHI sensitivity factors [35]. The peak positions were corrected for the charging effects by considering the C 1s peak at 285.0 eV and evaluating the BE differences [36].

XRD analyses were performed with a Bruker D8 Advance diffractometer with Bragg–Brentano geometry using a Cu $K\alpha$ radiation (40 kV, 40 mA, $\lambda = 0.154$ nm).

Temperature Programmed Reduction (TPR), and BET specific surface area measurements were performed with an Autochem II 2920 Micromeritics, equipped with a TCD detector. TPR measurements were carried out in a quartz reactor by using 50 mg of sample and heating from RT to 900 °C at 10 °C/min under a constant flow of H_2 5 % in Ar

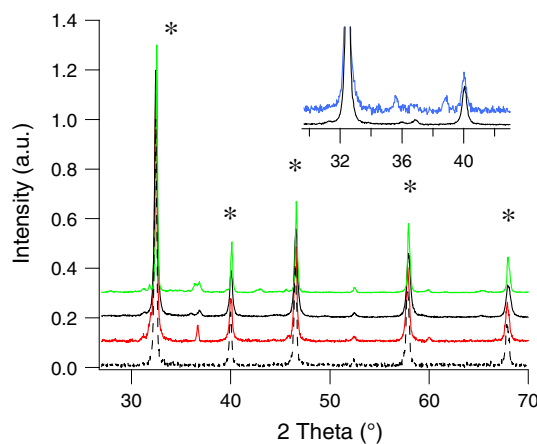
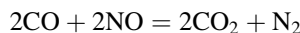
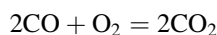


Fig. 1 XRD patterns obtained for SrTiO_3 (black dotted line); $\text{SrTi}_{0.7}\text{Co}_{0.3}\text{O}_3$ (black line); $\text{SrTi}_{0.7}\text{Cu}_{0.3}\text{O}_3$ (red line); $\text{SrTi}_{0.7}\text{Co}_{0.15}\text{Cu}_{0.15}\text{O}_3$ (green line). In the insets patterns of $\text{SrTi}_{0.7}\text{Co}_{0.3}\text{O}_3$ (black line) and of $\text{CuO}/\text{SrTi}_{0.7}\text{Co}_{0.3}\text{O}_3$ (blue line) are compared

(50 ml/min). The specific surface areas were determined (BET single point method) by means of N_2 adsorption at liquid nitrogen temperature on samples previously out-gassed at 350 °C in He.

2.3 Catalytic Tests

The catalysts were tested for the following reactions:



(feed compositions: 4 % CO + 2 % O_2 + He 94 % and 4 % CO + 4 % NO + He 92 %, respectively). The catalytic tests were carried out by loading about 40 mg of the sample in a “U” shaped glass reactor ($\text{GHSV } 42,000 \text{ h}^{-1}$); the temperature was checked by means of a thermocouple inserted into the reactor. The effluent gases from the reactor reached the GC (Agilent 7890 A equipped with TCD) for the analysis. Tests were performed between RT and 400 °C.

3 Results

3.1 Co and Cu-Doped SrTiO_3

XRD patterns obtained for $\text{SrTi}_{0.7}\text{Cu}_{0.3}\text{O}_3$, $\text{SrTi}_{0.7}\text{Co}_{0.3}\text{O}_3$, $\text{SrTi}_{0.7}\text{Co}_{0.15}\text{Cu}_{0.15}\text{O}_3$ (Fig. 1) indicate that the main phase is the perovskitic one; in the Cu-doped sample, however, traces of cubic CuO are also evident. This is consistent with the lower thermodynamic stability of the Cu-doped titanate, as predicted by Carlotto et al. [37]. The SEM

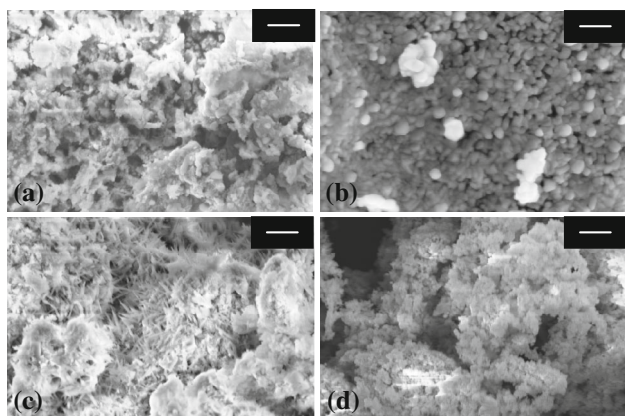


Fig. 2 SEM images obtained for the doped titanates: $\text{SrTi}_{0.7}\text{Co}_{0.3}\text{O}_3$ (a, b); for $\text{SrTi}_{0.7}\text{Cu}_{0.3}\text{O}_3$ (c) and for the impregnated $\text{CuO}/\text{SrTi}_{0.7}\text{Co}_{0.3}\text{O}_3$ (d). The line corresponds to 1 μm in (a), (c), and (d) and to 200 nm in (b)

images reveal a different morphology in the Co- and Cu-doped samples. The morphology of the Co-doped SrTiO_3 is rather homogeneous and characterized by a globular structure. In the Cu-doped SrTiO_3 , a less homogeneous morphology is evident. The particle dimensions range from 30 to 40 nm (Fig. 2). The BET specific surface area is 18 m^2/g for $\text{SrTi}_{0.7}\text{Cu}_{0.3}\text{O}_3$, and $\text{SrTi}_{0.7}\text{Co}_{0.15}\text{Cu}_{0.15}\text{O}_3$, and 20 m^2/g for $\text{SrTi}_{0.7}\text{Co}_{0.3}\text{O}_3$.

XPS spectra obtained for the different catalysts are compared in Figs. 3 and 4. The Ti $2p_{3/2}$ XPS signal is centred at 458.0 eV, the typical position of titanium in titanates, both in the undoped and in the Co-doped samples. A slight shift can be observed as a consequence of the Cu doping (458.5 eV) suggesting the slight increment of surface hydroxyl groups (Fig. 3c).

The Sr 3d signal in the undoped and Co-doped samples, is centred at 133–134 eV, a value slightly higher than the one expected for the Sr in SrTiO_3 (132.8–133.0 eV) that suggests the presence, besides perovskite, of SrCO_3 . Moreover, the peak shifts toward higher BE (134.7 eV) when copper is present suggesting the presence of strontium oxides and hydroxides [38, 39]. The O 1s peak shows two contributions due to the perovskite (529.5 eV) and to the hydroxyl/carbonate species (531.8–532.0 eV). The signal due to the surface contaminants increases in the doped catalysts. Particularly interesting are the signals due to cobalt and copper (Fig. 4). In the Co-doped sample the peak position (780.9 eV) and shape (absence of the shake-up contribution at about 785 eV) are consistent with the presence of Co(III). In $\text{SrTi}_{0.7}\text{Cu}_{0.3}\text{O}_3$ the Cu 2p peak position (933.2 eV) and the absence of the shake-up signal (at about 942–943 eV), suggest the presence of Cu(I).

The atomic composition (Table 1) reveals an oxygen overstoichiometry that confirms the surface hydroxyl/

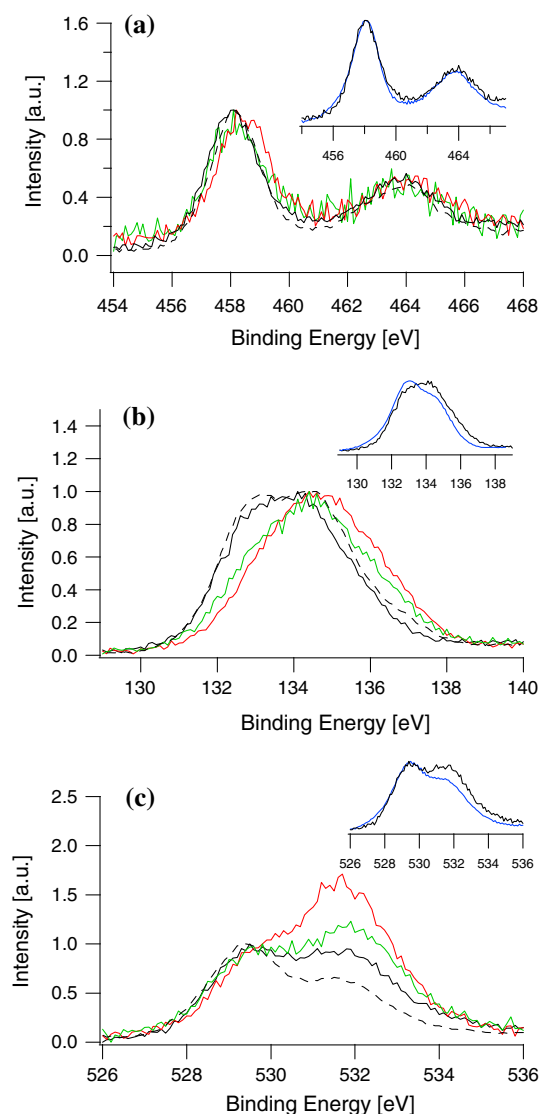


Fig. 3 XPS spectra obtained for: SrTiO_3 (black dashed line), $\text{SrTi}_{0.7}\text{Co}_{0.3}\text{O}_3$ (black line); $\text{SrTi}_{0.7}\text{Cu}_{0.3}\text{O}_3$ (red line); $\text{SrTi}_{0.7}\text{Co}_{0.15}\text{Cu}_{0.15}\text{O}_3$ (green line); in the inserts the spectra of $\text{CuO}/\text{SrTi}_{0.7}\text{Co}_{0.3}\text{O}_3$ (blue line); and $\text{SrTi}_{0.7}\text{Co}_{0.3}\text{O}_3$ (black line) are compared. a Ti 2p; b Sr 3d; c O 1s

carbonate contamination. Moreover, the comparison with the nominal composition, determined from the weighted amounts, suggests that Sr surface segregation occurs in the Cu-doped samples. It is also evident the different behaviour between the Co-doped and Cu-doped samples: cobalt is surface segregated whereas copper is highly depleted from the surface.

TPR results are displayed in Fig. 5. The profile of $\text{SrTi}_{0.7}\text{Co}_{0.3}\text{O}_3$ shows two well evident peaks at about 400 and 700 $^{\circ}\text{C}$ corresponding to the reduction of Co(III) to Co(II) and of Co(II) to Co(0), respectively. Another signal at lower temperatures (around 200 $^{\circ}\text{C}$) suggests the presence of an easy accessible cobalt (III) species Concerning

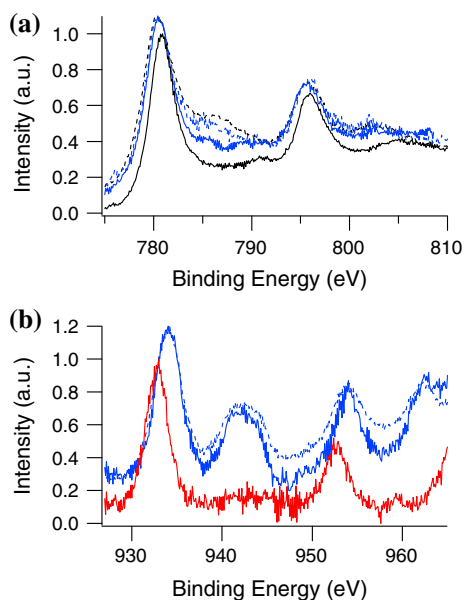


Fig. 4 XPS spectra of Co 2p (a) and Cu 2p (b) obtained for: SrTi_{0.7}Co_{0.3}O₃ (black line) SrTi_{0.7}Cu_{0.3}O₃ (red line); and CuO/SrTi_{0.7}Co_{0.3}O₃ (blue line). The spectra obtained on the catalysts after reaction (CO + 1/2O₂ for 9 h at 400 °C: black dotted line; CO+NO for 9 h at 400 °C: blue dotted line) are also reported

Table 1 XPS and nominal (N) atomic composition determined for the doped-titanates as a function of doping; the XPS atomic composition obtained after reaction (AR) is also reported for comparison: SrTi_{0.7}Co_{0.3}O₃ (CO oxidation) and CuO/SrTi_{0.7}Co_{0.3}O₃ (NO reduction)

Sample	Sr	Ti	Cu	Co	O
SrTi _{0.7} Cu _{0.3} O ₃					
XPS	25.1 (75.8)	7.4 (22.4)	0.6 (1.8)		66.9
N	20.0 (50.0)	14.0 (35.0)	6.0 (15.0)		60.0
SrTi _{0.7} Co _{0.3} O ₃					
XPS	15.7 (46.2)	8.7 (25.6)		9.6 (28.2)	66.0
AR	16.5 (45.2)	10.0 (27.4)		10.0 (27.4)	63.5
N	20.0 (50)	14.0 (35.0)		6.0 (15.0)	60.0
SrTi _{0.7} Co _{0.15} Cu _{0.15} O ₃					
XPS	21.7 (64.6)	4.5 (13.4)	0.6 (1.8)	6.8 (20.2)	66.4
N	20.0 (50.0)	14.0 (35.0)	3.0 (7.5)	3.0 (7.5)	60.0
CuO/SrTi _{0.7} Co _{0.3} O ₃					
XPS	16.8 (50.0)	9.5 (28.3)	2.0 (5.9)	5.3 (15.8)	65.6
AR	15.4 (41.6)	9.5 (25.7)	8.1 (21.9)	4.0 (10.8)	63.1
N	15.8 (43.4)	11.1 (30.4)	4.8 (13.1)	4.8 (13.1)	63.5

Inside brackets the atomic composition obtained only considering cations

SrTi_{0.7}Co_{0.15}Cu_{0.15}O₃ a general decrease of the intensity of the signals due to cobalt is observed. Moreover, the Co(II) to Co(0) reduction temperature decreases from 700 to 580–600 °C. Only two small signals around 450 and

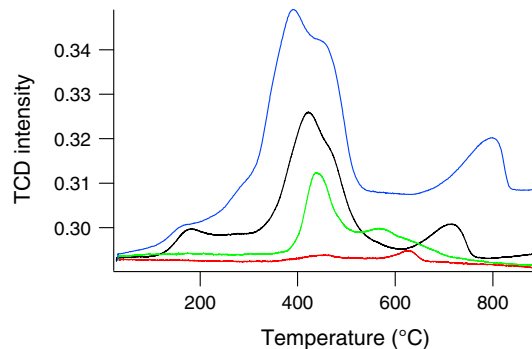


Fig. 5 TPR curves obtained: SrTi_{0.7}Co_{0.3}O₃ (black line); SrTi_{0.7}Cu_{0.3}O₃ (red line); SrTi_{0.7}Co_{0.15}Cu_{0.15}O₃ (green line); CuO/SrTi_{0.7}Co_{0.3}O₃ (blue line)

Table 2 Experimental (Exp) and estimated (Ext) (TPR) hydrogen consumptions measured for the doped-titanates as a function of doping

Sample	Exp (mol/mol)	Ext (mol/mol)	Exp/Ext
SrTi _{0.7} Co _{0.3} O ₃	0.39	0.45	0.87
SrTi _{0.7} Cu _{0.3} O ₃	0.03		
Cu (II)		0.30	0.10
Cu (I)		0.15	0.20
SrTi _{0.7} Co _{0.15} Cu _{0.15} O ₃	0.16	0.38	0.42
CuO/SrTi _{0.7} Co _{0.3} O ₃	0.79	0.75	1.05

600 °C corresponding to the two steps reduction of copper are observed in the SrTi_{0.7}Cu_{0.3}O₃.

The comparison between the experimental (TPR) and nominal hydrogen consumptions (Table 2) reveals for the SrTi_{0.7}Co_{0.3}O₃ catalyst a slightly lower value that agrees with the residual presence of Co(II) into the powder bulk.

On increasing the copper content the difference between the theoretical and experimental consumption becomes more and more evident. In literature it is reported that copper cations reduction depends on the A-cation, and it is particularly difficult if A=Sr [29].

SrTi_{0.7}Cu_{0.3}O₃, SrTi_{0.7}Co_{0.3}O₃, and SrTi_{0.7}Co_{0.15}Cu_{0.15}O₃ catalysts were investigated for the reactivity with respect to CO+1/2O₂ and CO+NO.

The CO conversion in the reaction with CO + 1/2O₂ reaches 90 % at 350 °C on SrTi_{0.7}Co_{0.3}O₃, whereas the values are lower for SrTi_{0.7}Cu_{0.3}O₃, and SrTi_{0.7}Co_{0.15}Cu_{0.15}O₃ (13, and 26 %, respectively at 400 °C) (Fig. 6). In contrast, no activity was observed in the NO reduction. The comparison with the XPS and TPR results suggests that the absence of activity in reduction could be attributed to the low amount of copper present on the catalyst surface and to its low reducibility. To better investigate this aspect, copper oxide was deposited on the surface of the catalyst more active in the oxidation reaction: SrTi_{0.7}Co_{0.3}O₃.

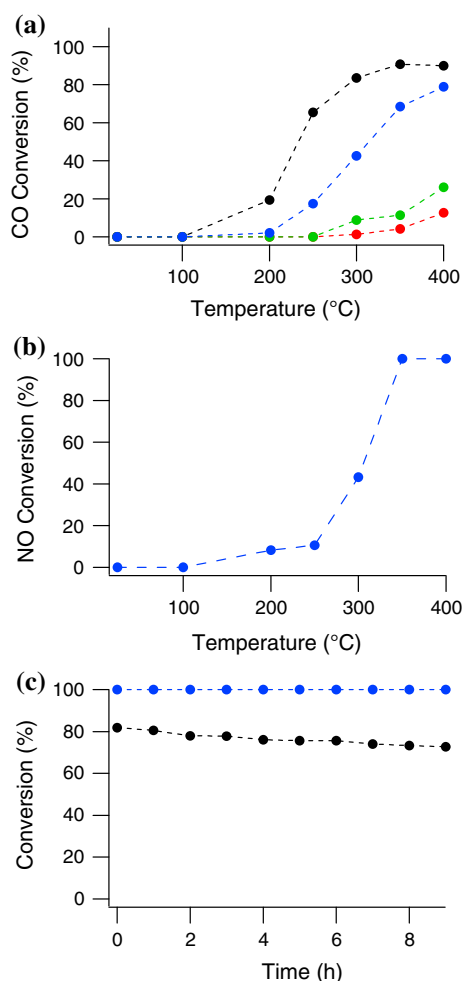


Fig. 6 Conversion values obtained for: SrTi_{0.7}Co_{0.3}O₃ (black); SrTi_{0.7}Cu_{0.3}O₃ (red); SrTi_{0.7}Co_{0.15}Cu_{0.15}O₃ (green); and for the CuO/SrTi_{0.7}Co_{0.3}O₃ (blue); **a** in CO oxidation; **b** in NO reduction; **c** durability test carried out (at 400 °C) considering the reactivity of SrTi_{0.7}Co_{0.3}O₃ in CO oxidation (black) and of CuO/SrTi_{0.7}Co_{0.3}O₃ in NO reduction (blue)

3.2 CuO/Co-Doped SrTiO₃

The XRD pattern reveals, beside the perovskite, the formation of cubic CuO (Fig. 1, inset). Concerning BET surface area, no significant variations are observed after copper oxide deposition. Also morphology is not affected by copper oxide deposition (Fig. 2d).

Concerning the XPS results, the main difference with respect to the supporting titanate concerns the copper spectral region. The Cu 2p_{3/2} peak position (934.1 eV) and shape are consistent with how expected for Cu(II) in CuO. Consistently the shake up signals (about 942 and 962 eV) are evident.

The cations-only composition suggests the surface segregation of Sr and Co. The amount of copper, in contrast, is lower than the nominal value suggesting the diffusion of this element inside the perovskite.

In TPR curve of CuO/SrTi_{0.7}Co_{0.3}O₃, (Fig. 5), two main signals are evident around 400 (Cu(II) to Cu(0) and Co(III) to Co(II)) and 800 °C (Co(II) to Co(0)) whereas a shoulder is observed at about 300 °C. The low temperature contribution already determined in the substrate before the impregnation is still evident at about 200 °C. It is interesting to observe the behaviour of copper which is reduced in a single step when present as CuO and in a two step process when inserted into the perovskite structure. This behaviour, already revealed in copper doped manganites and cobaltates, depends on the amount of dopant: when copper is present in low amount it follows the behaviour of the main B cation whereas a different TPR result was observed in copper rich perovskites [40]. The comparison between the estimated and measured consumption (Table 2) suggests that, in this case, cobalt is present as Co(III) and copper as Cu(II), and both these cations are completely reduced.

The CO conversion (Fig. 6) in the reaction with CO + NO reaches 100 % at 350 °C; the conversion in CO oxidation only slightly decreases (from 90 to 80 % at 400 °C) respect to SrTi_{0.7}Co_{0.3}O₃. The obtained results are particularly relevant if compared with those obtained in La-containing perovskites.

Several La-containing perovskites have been investigated as catalysts for TWC reactions considering the reaction between NO and CO or between NO and hydrocarbons. Among these the more significant are LaFeO₃ [15], LaCoO₃ [16, 17], LaMnO₃, [19, 20, 22, 41, 42]. As a general consideration doping is fundamental to obtain interesting NO conversions. The NO conversion in CO assisted reduction, as an example, is 21 % at 451 °C for LaFeO₃ but increases reaching 76–84 % when doping in the La site (with alkali elements) and in the Fe site (with copper, as an example) [23]. Similar considerations hold for LaCoO₃ and LaMnO₃. In this contribution the composite catalyst was obtained by combining the capability of perovskites to disperse and stabilize the copper oxide particles (which is fundamental for activity and selectivity [43] with the catalytic activity in CO oxidation of the doped titanate thus obtaining a double functionality.

3.3 Durability Tests

The reactivity of titanate based catalysts was investigated as a function of time at 400 °C. In particular SrTi_{0.7}Co_{0.3}O₃ was tested in CO oxidation whereas the composite CuO/SrTi_{0.7}Co_{0.3}O₃ was studied in the NO reduction. The reactivity of the composite with respect to NO does not decrease with time (Fig. 6c) whereas the CO conversion on SrTi_{0.7}Co_{0.3}O₃ decreases of about 5 % in 9 h.

As it can be observed in Table 1, the cobalt amount does not change after the CO oxidation; however, the

comparison between the Co 2p signal observed before and after the reaction (Fig. 4) is consistent with the cobalt reduction. In the spectrum after reaction, in fact, the shake-up structure characteristic of the Co(II) (around 785 eV) is more evident.

In contrast to that, no significant change is observed for the shape of the Cu 2p peak after NO reduction (Fig. 4), even though qualitative analysis show (see Table 1) that the quantity of copper increases.

4 Conclusions

In this manuscript several cobalt and copper doped catalysts have been prepared by means of the “citrate route”: $\text{SrTi}_{0.7}\text{Cu}_{0.3}\text{O}_3$, $\text{SrTi}_{0.7}\text{Co}_{0.3}\text{O}_3$, $\text{SrTi}_{0.7}\text{Co}_{0.15}\text{Cu}_{0.15}\text{O}_3$. XRD confirms the formation of the perovskite phase at 950 °C; the particle dimensions range around 30–40 nm, as revealed by SEM. The sample morphology changes with the doping: a homogeneous globular morphology is observed in the Co-doped titanate whereas a higher heterogeneity is evident in the Cu-doped sample.

XPS reveals that surface contamination increases with increasing the copper content; moreover in the Cu-doped sample strontium is surface segregated whereas in the Co-doped sample the segregation phenomenon mainly concerns cobalt.

$\text{SrTi}_{0.7}\text{Co}_{0.3}\text{O}_3$ is very active in the CO oxidation reaction (90 % at 350 °C) but the reactivity severely decreases when it is co-doped with copper; neither $\text{SrTi}_{0.7}\text{Co}_{0.3}\text{O}_3$ nor Cu-doped SrTiO_3 show activity in the NO + CO reaction.

When copper oxide is deposited on the $\text{SrTi}_{0.7}\text{Co}_{0.3}\text{O}_3$ surface, reactivity with respect to NO + CO (100 % NO conversion at 350 °C) greatly increases, whereas the reactivity in the CO oxidation reaction only slightly decreases.

The comparison between the obtained results underlines the different role played by copper and cobalt in the investigated reactions: cobalt, in fact, seems to be active in oxidation whereas copper is necessary for the reduction. Further investigations are in course for better understanding the reaction mechanism.

Acknowledgments The research leading to these results has received funding from the European Union’s 7th Framework Programme under grant agreement no 280890- NEXT-GEN-CAT. The authors gratefully acknowledge Dr. D. Lorenzi for his contribution.

References

- Libby WF (1971) *Science* 171:499
- Sorenson SC, Wronkiewicz JA, Sis LB, Wirtz GP (1974) *Bull Am Ceram Soc* 53:446
- Lisi L, Bagnasco G, Ciambelli P, De Rossi S, Porta P, Russo G, Turco M (1999) *J Solid State Chem* 146:176
- Simonot L, Garin F, Maire G (1997) *Appl Catal B* 11:167
- Seyfi B, Baghalha M, Kazemian H (2009) *Chem Eng J* 148:306
- Nitadori T, Kurihara S, Misono M (1986) *J Catal* 98:221
- Rajadurai S, Carberry JJ, Li B, Alcock CB (1991) *J Catal* 131:582
- Doshi R, Alcock C.B, Carberry JJ (1993) *Catal Lett* 18:337
- Song KS, Cui HX, Kim SD, Kang SK (1999) *Catal Today* 47:155
- Panich NM, Pirogova GN, Korosteleva RI, Voronin YV (1999) *Russ Chem Bull* 48:695
- Hirano T, Purwanto H, Watanabe T, Akiyama T (2007) *J Alloys Compd* 441:263
- Lee YN, Lago RM, Fierro JLG, Cortés V, Sapiña F, Martínez E (2001) *Appl Catal A* 207:17
- Peña MA, Fierro JLG (2001) *Chem Rev* 101:1981
- Ladavos AK, Pomonis PJ (1993) *Appl Catal B* 2:27
- Mescia D, Trikalitis PN, Ladavos AK, Bakas TV, Pomonis PJ (1999) *Appl Catal A* 177:53
- Simonot L, Garin F, Maire G (1997) *Appl Catal B* 11:181
- Ocal M, Oukaci R, Marcelin G, Agarwal SK (1994) *Ind Eng Chem Res* 33:2930
- Mizuno N, Tanaka M, Misono MJJ (1992) *Chem Soc Faraday Trans* 88:91
- Lindstedt A, Strömberg D, Abul-Milh M (1994) *Appl Catal A* 116:109
- Shen ST, Weng HS (1998) *Ind Eng Chem Res* 37:2654
- Wu X, Xu L, Yang B, Weng D (2004) *Surf Coat Techn* 184:40
- Wu X, Xu L, Weng D (2004) *Catal Today* 90:199
- Mescia D, Caroca JC, Russo N, Labhsetwar N, Fino D, Saracco G, Specchia V (2007) *Catal Today* 137:300
- Russo N, Fino D, Saracco G, Specchia V (2005) *J Catal* 229:459
- Liu F, He H, Zhang C, Feng Z, Zheng L, Xie Y, Hu T (2010) *Appl Catal B* 96:408
- Liu F, He H, Zhang C, Shan KW, Shi X (2011) *Catal Today* 175:18
- López-Suárez FE, Bueno-López A, Illán-Gómez MJ, Adamski A, Ura B, Trawczynski J (2008) *Environ Sci Technol* 42:7670
- López-Suárez FE, Illán-Gómez MJ, Bueno-López A, Anderson JA (2011) *Appl Catal B* 104:261
- Ura B, Trawczyński J, Zawadzki M, Illán-Gómez MJ, Bueno-López A, López-Suárez FE (2011) *Catal Today* 176:169
- Ura B, Trawczyński J, Kotarba A, Bieniasz W, Illán-Gómez MJ, Bueno-López A, López-Suárez FE (2011) *Appl Catal B* 101:169
- López-Suárez FE, Parres-Esclapez S, Bueno-López A, Illán-Gómez MJ, Ura B, Trawczyński J (2009) *Appl Catal B* 93:82
- Fabbrini L, Kryukov A, Cappelli S, Chiarello GL, Rossetti I, Oliva C, Forni L (2005) *J Catal* 232:247
- Oliva C, Bonoldi L, Cappelli S, Fabbrini L, Rossetti I, Forni L (2005) *J Mol Catal A* 226:33
- Shirley DA (1972) *Phys Rev B* 5:4709
- Moulder JF, Stickle WF, Sobol PE, Bomben KD (1992) In: Chastain J (ed) *Handbook of X-ray photoelectron spectroscopy*, Physical Electronics, Eden Prairie
- Briggs D, Riviere JC (1983) in: Briggs D, Seah MP (Eds.) *Practical Surface Analysis*, Wiley, New York
- Carlotto S, Natile MM, Glisenti A, Vittadini A (2013) *Chem Phys Lett* 588:102
- Natile MM, Poletto F, Galenda A, Glisenti A, Montini T, De Rogatis L, Fornasiero P (2008) *Chem Mater* 20:2314
- Galenda A, Natile MM, Krishnan V, Bertagnolli H, Glisenti A (2007) *Chem Mater* 19:2796
- Glisenti A, Galenda A, Natile MM (2013) *Appl Catal A* 453:102
- Mizuno N, Tanaka M, Misono MJ (1992) *J Chem Soc Faraday Trans* 88:91
- Wu X, Xu L, Yang B, Weng D (2004) *Surf Coat Tech* 184:40
- Amano F, Suzuki S, Yamamoto T, Tanaka T (2006) *Appl Catal B* 64:282